



Spatio-temporal Analysis of Precipitation and Temperature: A Case Study Over the Beijing–Tianjin–Hebei Region, China

BAOHUI MEN,¹ ZHIJIAN WU,¹ HUANLONG LIU,¹ WEI TIAN,² and YONG ZHAO³

Abstract—Climate change have a profound impact on the production and life of the people in the Beijing–Tianjin–Hebei region. Precipitation and temperature are regarded as two basic components of climate. This study investigated the spatial and temporal characteristics of precipitation and temperature over the region from 1960 to 2013. Different methods were used to analyze temporal variation and the results are mutually verified. Wavelet analysis was adopted to analyze the abrupt changes of precipitation and temperature. Empirical orthogonal function decomposition method was utilized to analyze the spatial distribution of temperature and precipitation. The study yielded three major findings: First, the inter-annual decrease and increase of precipitation appeared alternately in the region. Temperature was rising significantly in the last 50 years, apart from a slow reduction in the late 1970s. Second, the spatial distribution characteristics of precipitation vary due to the distance from the ocean. The increasing trend of temperature in Beijing-centered region was more obvious than that in areas away from the sea. Third, precipitation and temperature show strong correlations in change. When temperature increased, the rainfall decreased. What is more, when the temperature mutated, the precipitation also changed rapidly. The results can guide local agriculture production and provide reference for the further study of climate change.

Keywords: Beijing–Tianjin–Hebei region, Temperature, Precipitation, Temporal and spatial distribution.

1. Introduction

Temperature and precipitation are two basics climatic factors. According to the Intergovernmental Panel on Climate Change (IPCC 2013), the global mean surface temperature has increased by 0.85 °C from 1880 to 2012. Recent climate change has led to increased variability of the hydrological cycle at a global scale, creating uncertainty regarding predicting future climate conditions and associated impacts (Kharin et al. 2013; Lee et al. 2013; Zhang et al. 2014). The changes both in extreme temperature and mean temperature have already affected the physical and biological systems on all continents (Västilä et al. 2010; Pavlik et al. 2012; Zhou et al. 2014).

Therefore, an increasing number of experts and scholars began to pay attention to regional temperature and precipitation changes in recent years. Studies on precipitation and temperature variability have used various statistical methods, such as soil and water assessment tool (Golmohammadi et al. 2017), Kolmogorov–Smirnov (KS) two-sample test (Loukas and Quick 1996), Mann–Kendall test (Yang et al. 2017) and EOF analysis (Wang et al. 2013; Zhang et al. 2014). From a global point of view, seasonal precipitation trends based on month varied, with the summer and autumn series showing the largest significant increases in the upper Tennessee Valley (Jones et al. 2015). Further, Mann–Whitney test was used for probable break point detection in the series in India. The results indicated decreasing annual and monsoon rainfall of India in most of the sub-divisions (Kundu et al. 2015). From the point of view of research methods, it is necessary to adopt more reliable interpolation method and spatial model according to the research direction of the user when

¹ Beijing Key Laboratory of Energy Safety and Clean Utilization, North China Electric Power University, Renewable Energy Institute, Beijing 102206, China. E-mail: menbh@ncepu.edu.cn; 1172211088@ncepu.edu.cn; liuhuanlongHD@163.com

² Key Laboratory of Water Cycle and Related Land Surface Process, Institute of Geographic Sciences and Natural Resources Research, Chinese Academy of Sciences, Beijing 100101, China. E-mail: tianweiBT@163.com

³ State Key Laboratory of Simulation and Regulation of Water Cycle in River Basin, China Institute of Water Resources and Hydropower Research, Beijing 100038, China. E-mail: iwhrzhy@sohu.com

analyzing the daily variation of precipitation in a region (Paola and Giugni 2013; Safavi et al. 2016). Although a variety of research methods have been put forward and adopted, few research methods combine the advantages of different research methods and prove each other.

As for China, the temperature in the Hexi Corridor area had a significant upward trend in the past 57 years, whereas the increasing trend of precipitation in all the basins is not evident (Meng et al. 2013; Qian et al. 2016). EOF was used to analyze precipitation data in Shaanxi Province, indicating that there were six types of precipitation in Shaanxi Province. The southern part was rainy, but the north was just opposite (Qiu et al. 2011; Jiang et al. 2016). Analysis of the results obtained by the EOF method in coastal areas requires full consideration of the effects of monsoons and atmospheric pressure. Wet and dry areas of China had different extreme value of precipitation. (Ge et al. 2015). Shi et al. (2015) investigated the spatial and temporal characteristics of precipitation over the Three-River Headwater region during 1961–2014. The results indicated that the mean annual precipitation in region showed a southeast-to-northwest decreasing trend.

However, almost no research of temperature and precipitation was studied in Beijing–Tianjin–Hebei region. Besides, these studies usually adopted one or two methods and ignored the mutual verification between different methods. This reduced the reliability of the research to some extent. Qin et al. (2015) used the Soil Moisture Drought Severity and Standardized Precipitation Index to evaluate drought severity in Haihe basin. Results indicated that there was a significant increasing trend in the drought-affected area, and that the drought in 1999 had the greatest influence. Therefore, it is important and necessary to provide guidance for local agricultural production and reference for studies on global warming through the study of the temporal and spatial variation of precipitation and temperature in the region.

This paper used the daily precipitation and temperature data from 25 weather stations in the Beijing–Tianjin–Hebei region from 1960 to 2013 to achieve following objectives: (1) to study the tendency of precipitation and temperature on different scales and

analyze whether there are abrupt changes in precipitation and temperature in the 54 years. If there are, figure out the time of abrupt change. (2) To analyze the spatial variation of temperature and precipitation, (3) to study the relationship between precipitation and temperature in this area. (4) To enable each method to prove each other, especially when studying the trend of precipitation or air temperature.

2. Study Area

Connected by the Eurasian continent and the Pacific Ocean, Beijing–Tianjin–Hebei region is the capital region in the northern China including 11 prefecture-level cities (see Fig. 1). Influenced by warm temperate monsoon climate, the area has four distinct seasons. The regional difference of precipitation is also obvious. The analysis of climate change in this region may help local people better address climate change and improve haze prevention and control.

3. Data and Methods

3.1. Data

This study used the daily weather and precipitation data of from weather stations in the Beijing–Tianjin–Hebei region from 1960 to 2013. Because the data of each station was the point rainfall data, this study transformed point into surface with the Tyson polygon method and get the surface rainfall of the area monitored by each station (see Table 1). Tyson polygon method is a common method for the transformation of point to surface rainfall, which is to connect all adjacent weather stations into a triangle and connect the intersections of the vertical bisectors of the three sides of each triangle to obtain a polygon. Using the rainfall intensity of a unique weather station contained in this polygon represent the rainfall intensity in this polygonal region.

It can be seen from the above table that the average rainfall calculated by the Tyson polygon method is more accurate. Therefore, we will use the Tyson polygon method to calculate the annual

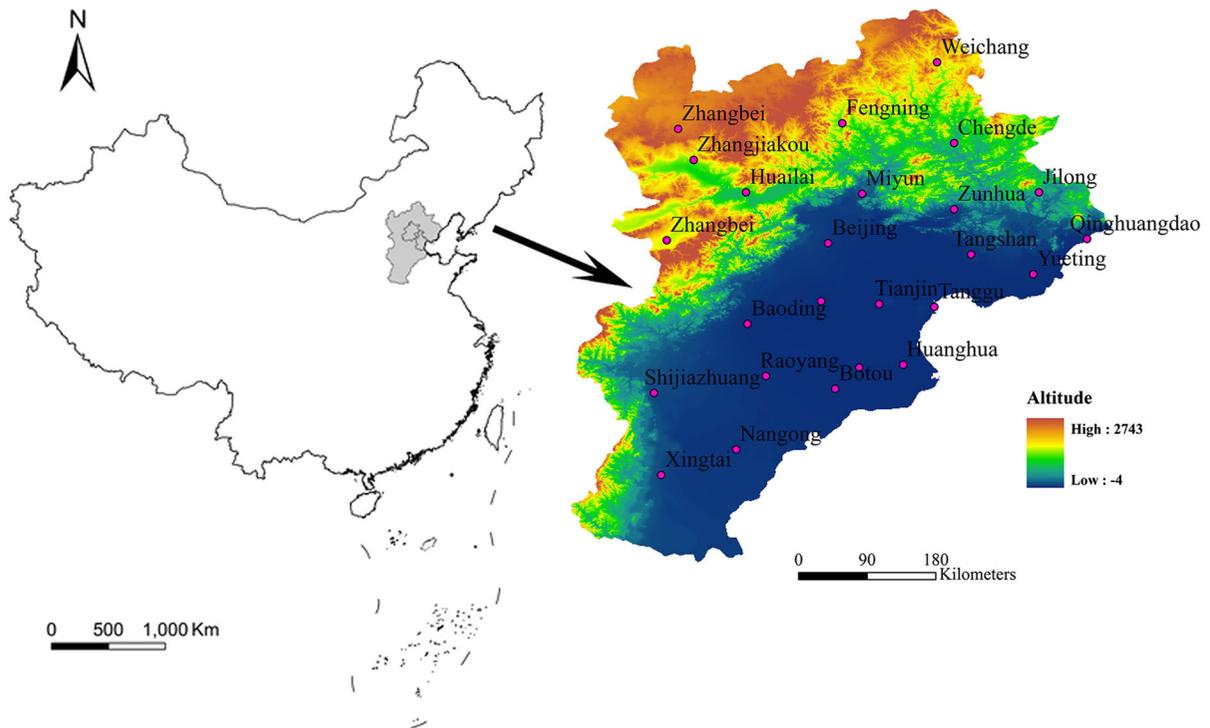


Figure 1
Location of Beijing–Tianjin–Hebei region and weather stations

Table 1

Comparison of point-to-surface rainfall conversion under Tyson polygon conditions

Representative years	Frequency (%)	Thiessen polygon (mm)	Isoline (mm)	Error in thiessen polygon (%)
1990	90	645.84	668.61	3.41
1966	75	553.18	572.47	3.37
1971	50	503.56	520.01	3.16
1993	25	457.18	464.08	1.49

precipitation sequence in the analysis of the inter-annual variation of rainfall.

3.2. Methods

3.2.1 Methods for Trend Analysis

In this study, linear regression, slip averaging of five-year, ensemble empirical mode decomposition (EEMD), cumulative anomaly method and R/S analysis were used to analyze temporal trends of

precipitation and temperature. All kinds of analytical methods confirm each other to ensure the accuracy and reliability of the results.

Unitary linear regression is the simplest and easiest way to see the analysis of sequence trends. Slip averaging can reflect the continuity of the data in the time series, effectively reduce the influence of data fluctuating and reflect the stage change more intuitively. Cumulative anomaly method requires getting the average of the series, then adds the difference between the series and the mean of the cumulative series.

EEMD not only retains the information of the original sequence, but also overcomes the problem of modal confusion by adding white noise to the original sequence. EEMD is an improvement on the empirical mode decomposition (EMD) (Cheng et al. 2011; Wang et al. 2012). EMD divides the time series into a series of IMFs. EEMD adds a different white noise process in original sequence and repeats n times. The average of the IMF of n times is taken as the final IMF component.

The R/S method is proposed by Hurst and other hydrological workers on the basis of a large number of empirical studies. It is effective to prove the continuity of changes and to allow a quantitative comparison of component intensities.

3.2.2 Methods for Spatial Analysis

EOF was used to analyze the spatial distribution of rainfall and temperature. EOF method decomposes the variable field matrix with time as two mutually orthogonal matrices by means of dimensionality reduction, which can reflect the original characteristics of the variable field and quickly enrich the large amount of information of the original variable field into few comprehensive indexes (Small and Islam 2006). The large amount of information of the original variable field is condensed into a few comprehensive indexes to decompose the irregularly distributed sites, and reduced the impact of time on space research (Xie et al. 2003).

3.2.3 Methods for Abrupt Change Analysis

The Mann–Kendall test and cumulative anomaly method were used to explore the abrupt changes of precipitation and temperature series (Mondal et al. 2014). Then, nonparametric tests were performed on the data before and after the abrupt change points of temperature. The Mann–Kendall test has the advantage of not assuming any distribution form for the data and has similar power to its parametric counterparts. In the absence of a trend in the series, the graphical representation of $UF(t)$ and $UB(t)$ will intersect several times. For this study the confidence interval was taken as ± 1.96 ($p = 0.05$). If the intersection is at the critical horizontal line corresponding to the confidence level, the point maybe the abrupt point. The research route of this paper was as follow (see Fig. 2).

4. Results and Discussion

4.1. Temporal Trend of Precipitation and Temperature

Based on the daily precipitation collected from 25 weather stations from 1960 to 2013, the cumulative

average method was used to analyze the annual average precipitation and the linear trend line and the 5-year moving average method were adopted to study the overall trend of the temperature change. In addition, the R/S method was used to analyze the persistence of precipitation and temperature change. The multiple R/S values were averaged to obtain a series of corresponding $\log(R/S)$ and $\log(r)$, and the Hurst exponent was obtained by least-squares method (see Fig. 3).

From Fig. 3a, we can see that the group of wet year and dry year occurred alternately. The lowest point was in 2007, but the highest was in 1996. In general, the precipitation change can be divided into four stages: 1960–1979, 1993–1996, corresponding to the wet season and 1979–1993, 1996–2007, corresponding to dry season. Specifically, the frequency of change was high. Recently, it showed a downward trend with slight increase in the internal fluctuations in 1995–2013.

From Fig. 3b, the temperature was increasing at a rate of $0.26\text{ }^{\circ}\text{C}/10$ years from 1960 to 2013, which were consistent with the current state of global warming. Five-year moving average trend reflected that temperature alternately changed from cold to warm. The temperature showed a downward trend in the 1960s and began to rise slowly from the 1970s, and then experienced a slow decline in the 1980s. Until the late 1980s, there was a period of rapid rise in the area.

As can be seen from Fig. 3c, Hurst index was 0.5529, indicating the sequence's characteristics of continuous change, and showing that the downward trend of precipitation in the past 50 years will continue to exist in the next period.

The Hurst coefficient of temperature was 0.919 by the least square's method from the above figure. The Hurst coefficient was close to 1 and value of R^2 was 0.95, indicating that the sequence had a strong state persistence. According to the linear trend line fitting and the 5-year sliding trend, the temperature of the region would continue to rise in the future, and the upward trend in temperature would be very likely to persist for long periods of time.

This paper used EEMD to verify the trend of precipitation and temperature. From the

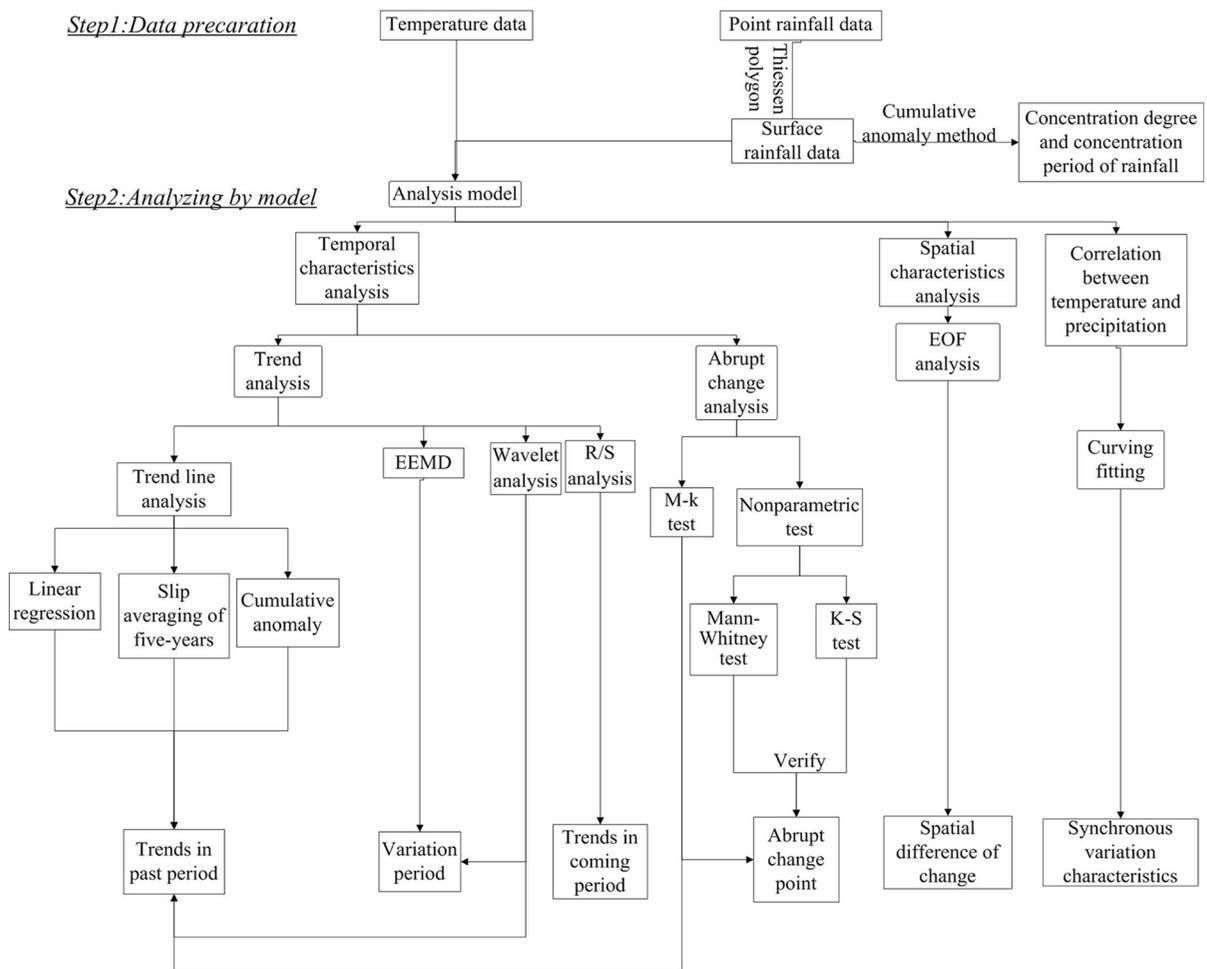


Figure 2 Research route of this paper

decomposition model of precipitation (see Fig. 4), the following information can be seen:

The annual precipitation sequence in the Beijing–Tianjin–Hebei region can be decomposed into four IMF components with different fluctuation periods and a trend component, indicating that the precipitation sequences contained multiple time scales.

Frequency and vibration of IMF1 was the largest in the four decomposed IMF. The amplitude fluctuated significantly around 1970 and 2000. The frequency of change was reduced and tended to be stable in the IMF3 and IMF4.

The trend term represented the trend of the overall precipitation sequence, and it can be seen that the

sequence increased firstly and then decreased over the whole-time scale.

This paper used fast Fourier transform to find the average period of each IMF component. The energy was mainly concentrated in the small scale of 3 years from the curve. Similarly, the cycles of the second, third and fourth largest energy components were 7 years, 18 years and 27 years respectively.

Similarly, to verify the accuracy of the study on the overall trend, this paper used EEMD method to analyze annual average temperature. The following conclusions were obtained by analyzing the intrinsic modal function and the trend term.

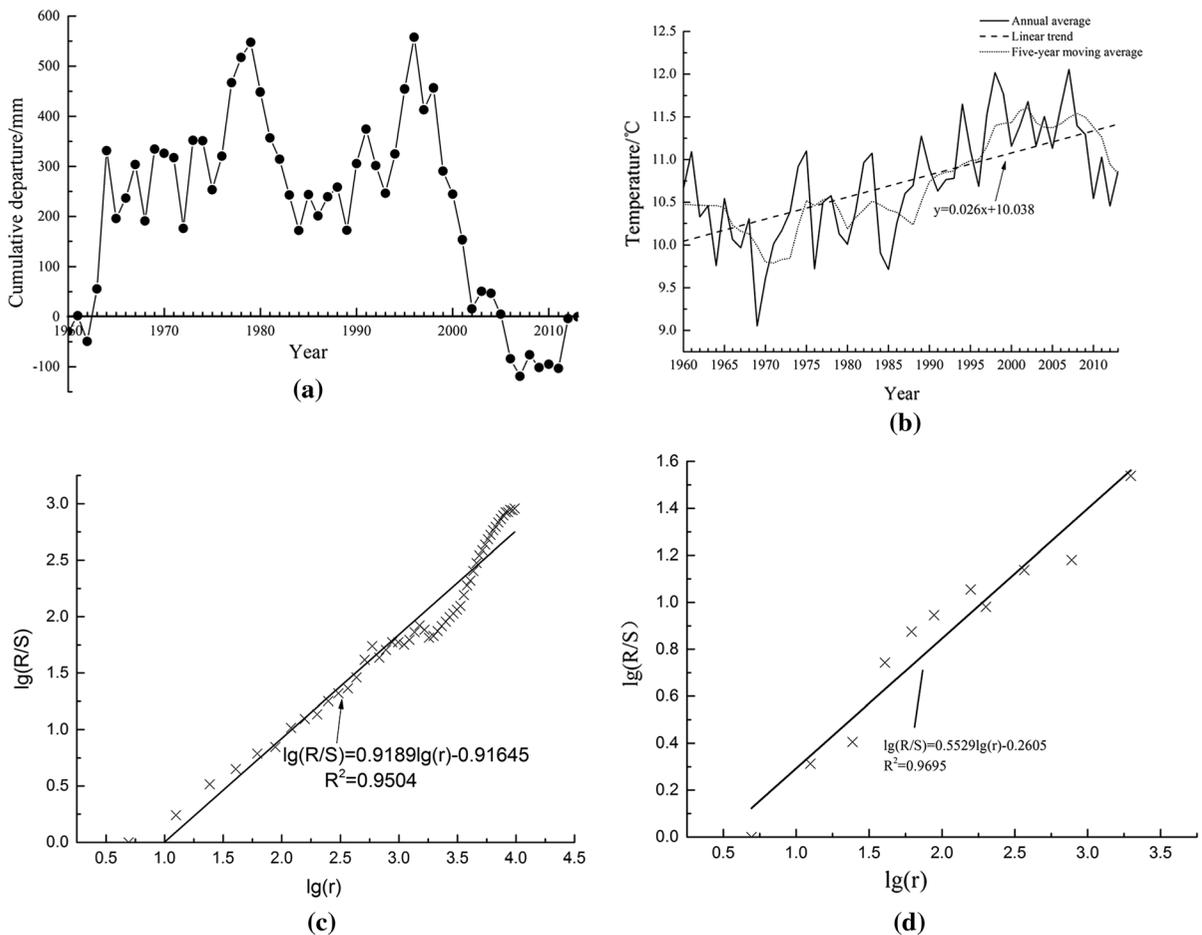


Figure 3

Temporal trend of precipitation and temperature. **a** Cumulative departure curve of precipitation, **b** temporal trend of annual average temperature, **c** R/S analysis of precipitation, **d** R/S analysis of temperature

The annual temperature sequence in the Beijing-Tianjin-Hebei region can be separated into four IMF components with a different fluctuation period and a trend component, indicating that the temperature sequence contained multiple time scales.

Frequency and vibration of IMF1 was the largest. The IMF1 fluctuated significantly around 1980 and 1990, indicating that the two periods had great possibility of sudden changes in temperature. IMF2 in the mid-1970s and in the mid-1980s fluctuated larger, indicating that the temperature change in these two periods were relatively large. IMF3 and IMF4 changed little and frequency tended to be stable.

This paper used fast Fourier transform to find the average period of each IMF component. The energy

was mainly concentrated in the small scale of 4 years from the curve, corresponding the period of 4 years. Similarly, the cycles of the second, and third and fourth largest energy component were 8 years, 14 years and 50 years respectively.

As time goes on, the average of the hydrological sequence may move slowly up or down over a long period of time. This paper used wavelet to analyze the trend of temperature change.

The real part of the wavelet coefficient contains both the time and the scale signal information. The size of the model represents the strength of the time scale signal. The larger the value of the module was, the more obvious the time and scale period were. The magic square can eliminate the false shock of the real

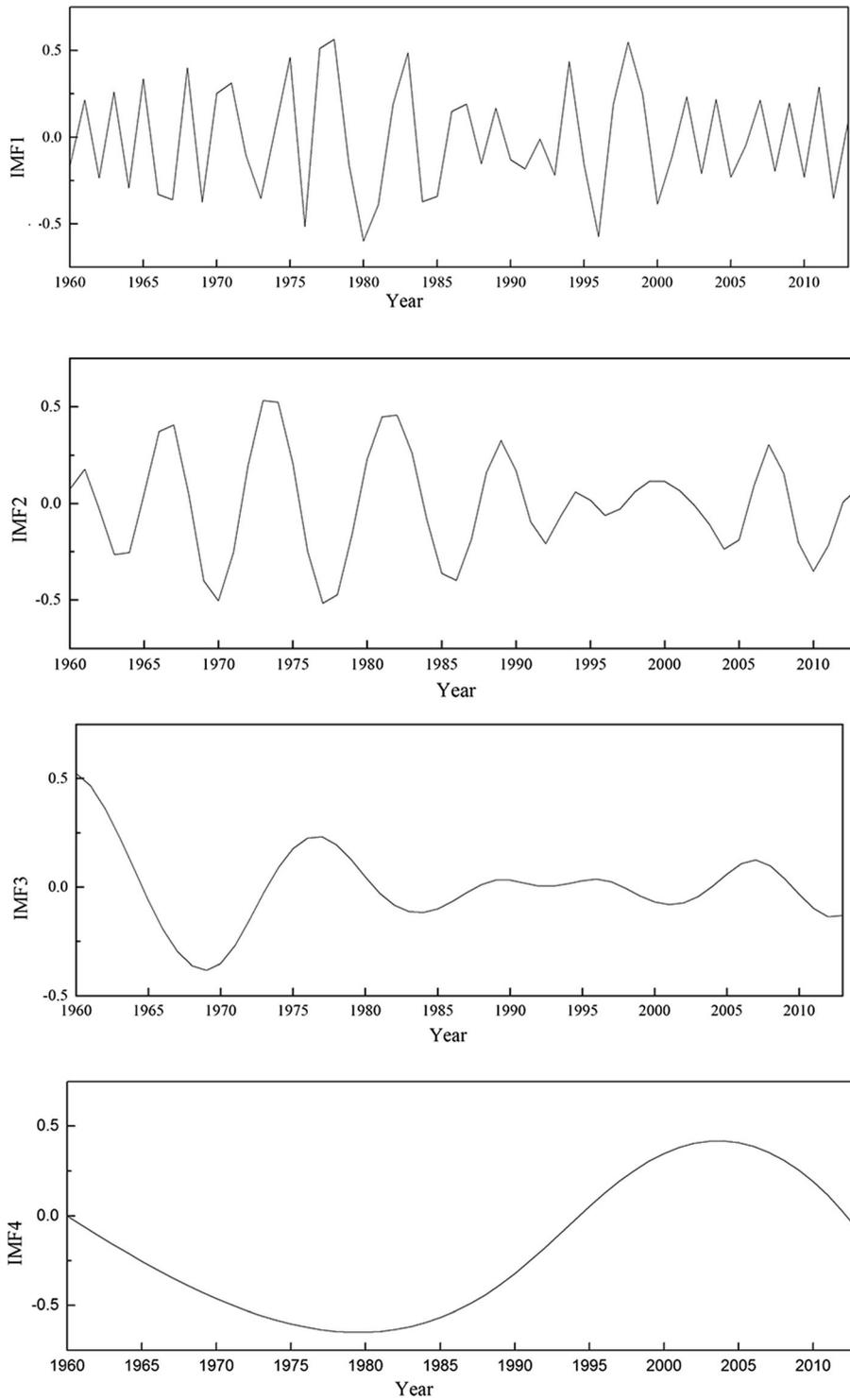


Figure 4
IMF of EEMD decomposition for precipitation

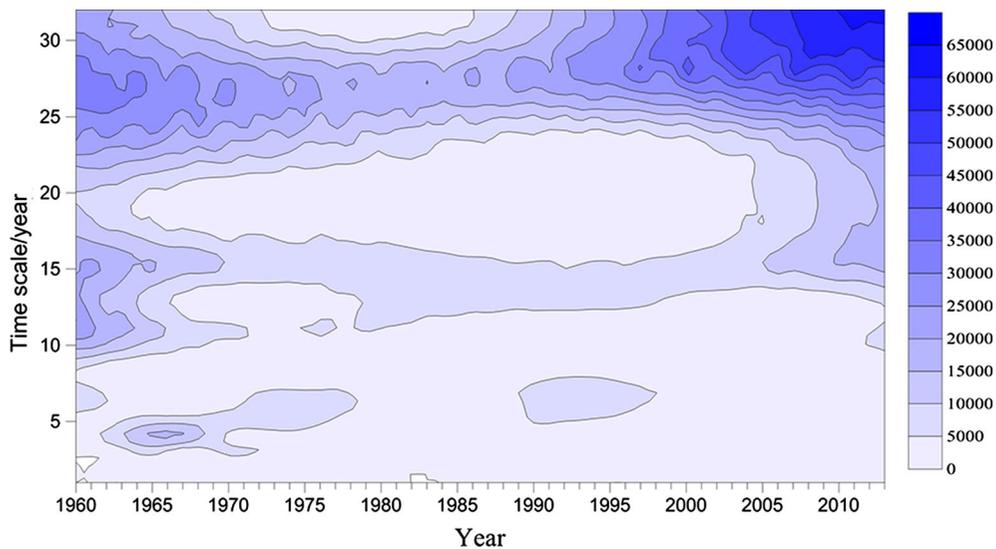


Figure 5
Mode squared distribution of wavelet transforms

wavelet, making the analysis more accurate. The contour map was drawn according to the square of the modulus square of the wavelet (see Fig. 5).

From the time–frequency distribution of Morlet wavelet transform coefficients, the inter-annual and inter-decadal characteristics of temperature change were obvious. The fluctuating energy almost ran through the entire time domain, and the scale ranged from 5 to 32 years. It can be divided into two stages by the end of the 1980s. The shock of first phase was in 1975 and the shock scale was 27 years. The shock of second phase was in 2010 and the shock scale was 30 years. The energy intensity in the time domain was concentrated after 1990, indicating that the temperature had a significant increase trend on this scale.

In addition, this paper studied the annual variation of precipitation by analyzing concentration degree and concentration period of the precipitation. Concentration degree reflects the degree of precipitation concentration in different research periods during the study period. Concentration period shows the time when the maximum precipitation occurs in a year. Both can well reflect the non-uniform temporal characteristics of the two in a certain process (see Fig. 6).

The concentration of precipitation was between 0.54 and 0.80, and the fluctuation became more intense after 1980s. In periods of 1960–1963, 1973–1978 and 1994–1996, the precipitation concentration was greater than the multi-year average, indicating that precipitation of these years was concentrated. On the contrary, precipitation was not concentrated in 1997–2004 and 2007–2010. From the inter-annual variability curve of precipitation concentration, the concentration period showed a decreasing trend in the fluctuation. Especially after 1979, most of the precipitation concentrated period was lower than the multi-year average, showing that the precipitation concentration appeared earlier every year.

4.2. Abrupt Change Analysis of Precipitation and Temperature

Based on the average annual sequence in the region, the Mann–Kendall (M–K) test method was used to analyze the abrupt change (see Fig. 7).

The results showed that the Z value of the average annual precipitation sequence was -0.5222 , indicating that the precipitation in this area showed a decreasing trend (see Fig. 7a). However, the Z value corresponding to the confidence level $\alpha = 0.05$ was

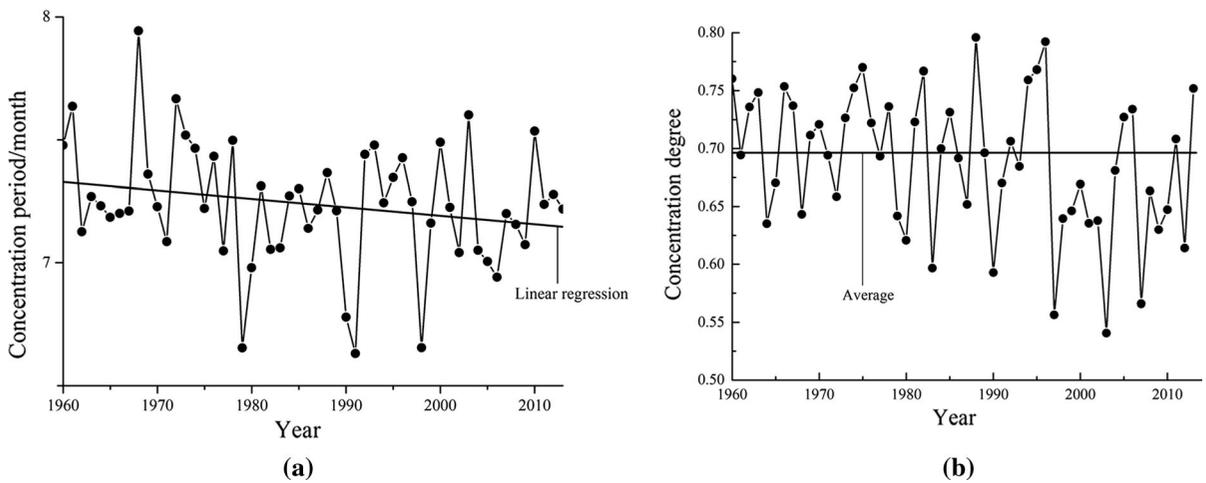


Figure 6

Concentration of precipitation. **a** Inter-annual variation curve of precipitation concentration period. **b** Inter-annual variation curve of precipitation concentration degree

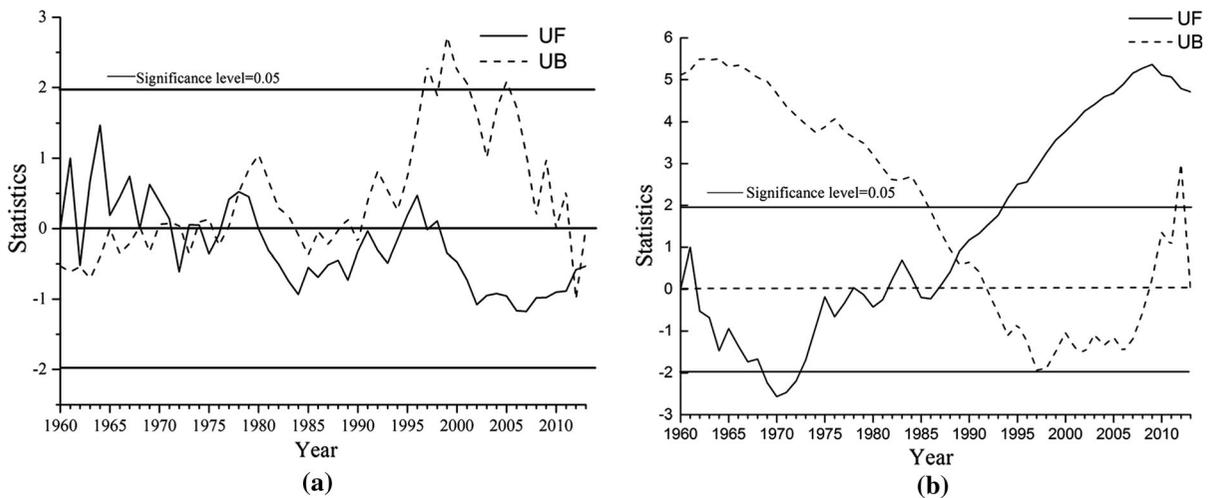


Figure 7

Result of M-K analysis. **a** M-K analysis of precipitation, **b** M-K analysis of temperature

1.96 and the *UF* value of the sequence was less than 1.96. The downward trend of precipitation was not obvious.

From 1968 to 1978, it can be seen from the above figure that the *UF* curve intersected the *UB* curve in several years. The intersection was within 0.05 significant horizontal intervals, so these years may be the time of the abrupt change. Further analysis showed that the precipitation began to change

abruptly after 1970s, which was consistent with the results of EEMD method. In the 2011 and 2012, *UF* curves and *UB* curves were intersected again, and the intersection was located within the confidence interval. It was expected that the precipitation in the next few years would change abruptly once again.

As for temperature (see Fig. 7b), the *UF* value exceeded the corresponding significance level of 0.05, showing a significant warming trend after the

1990s. *UF* and *UB* curves intersecting at two significant horizontal lines indicated that the temperature started changing abruptly from late 1980s and increased significantly after the abrupt point.

4.3. Spatial Variability of Precipitation and Temperature

In this paper, the spatial distribution was analyzed by EOF. The EOF method can better reflect the original features of the variable field, and quickly condensed the large amount of information in the original variable field into a few comprehensive indexes.

This paper selected three spatial sequences with the largest variance contribution after variance. The variance contribution rate reached 52.38%, 11.76% and 6.94% respectively. The cumulative contribution rate was 70.99%, which was highly representative. The results were as follows:

1. The variance contribution rate of modal 1 is 52.38%, which reflects the main characteristic form of precipitation change in the region. Consistency of all regions' symbols reflected the synchronicity of precipitation changes in the Beijing–Tianjin–Hebei region from 1960 to 2013. However, the value of eastern coastal areas was larger than that of western inland area. The maximum was distributed in Qinhuangdao–Tangshan–Tianjin–Cangzhou area, which indicated that the change of precipitation in eastern coastal areas was larger than that in western inland.
2. The value of modal 2 was decreasing from northeast to southwest. The northeast was positive and the southwest was negative. It was shown that there were differences between the change direction of northeast and the southwest.
3. The value of modal 3 was decreasing from the central region to the southeast and northwest and from the positive value to the negative value. It demonstrates that the changes of precipitation in the southeastern and northwest regions were occasionally different.

Above analysis indicated that the spatial distribution of precipitation can be characterized by three typical characteristics, namely, the coastal-inland

difference type, the northeast-southwest descending type and the gradually decreasing type from central to northwest and southeast. The coastal-inland difference was the main spatial distribution of regional precipitation, which corresponded to the temperate monsoon climate in the Beijing–Tianjin–Hebei region.

Similarly, the size of the eigenvalues reflected the degree of temperature change. According to the proportion of eigenvalue contribution rate, this paper took the first three eigenvectors. The accumulated contribution rate reached 91.92%, which reflected the main characteristics of spatial variation in the region (see Fig. 8).

Figure 8a was the first eigenvector of EOF decomposition, and its contribution rate was 82.65%. It was the main feature of the spatial distribution of air temperature. The eigenvalues were positive and showed consistency overall, indicating that the change of temperature was generally consistent. Deep color appeared in areas away from the ocean and areas that centered on Beijing and Tianjin. It was shown that temperature changed largely in the two regions, but changes were relatively small in other areas. The trend increased from the coast to the inland.

Figure 8b was the second eigenvector of EOF decomposition and its contribution rate was 6.68%. There were both positive and negative numbers in the picture, indicating that the characteristics of variation in some areas were opposite. This difference reflected the indication that temperature rose in some northern and eastern areas when that dropped in some southern areas.

Figure 8c was the third eigenvector of EOF decomposition, and its contribution rate was 2.59%. It is a form of occasional temperature spatial distribution. This distribution presented a distinct east–west difference.

4.4. Correlation Between Temperature and Precipitation

Based on the concept of regression association, the regression model was established by using annual precipitation and temperature data (see Fig. 9). Points in scatter plot were concentrated on both sides of the

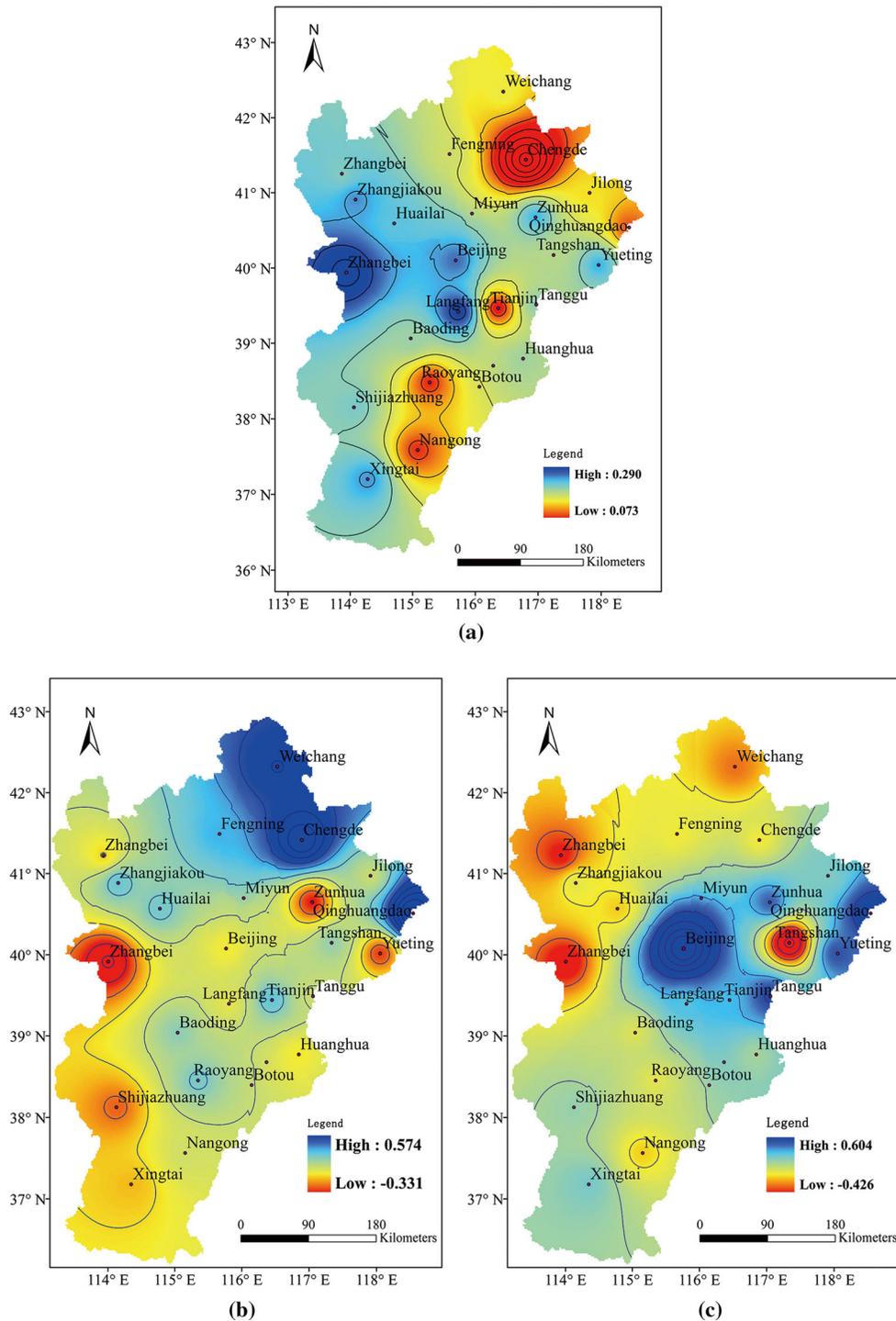


Figure 8

EOF decomposition of temperature. **a** The first eigenvector of EOF decomposition. **b** The second eigenvector of EOF decomposition. **c** The third eigenvector of EOF decomposition

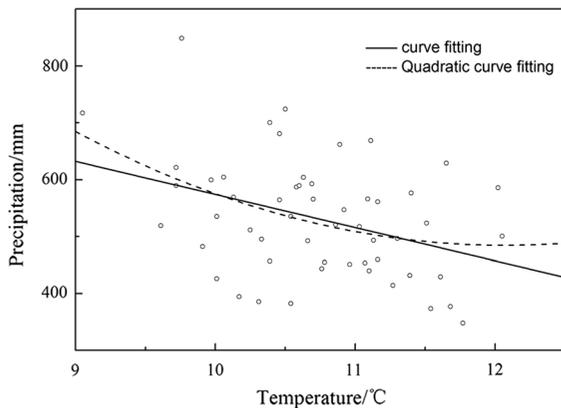


Figure 9

Correlation between precipitation and temperature

one fitting curve and the quadratic fitting curve. The correlation between temperature and precipitation in the two fitting methods went through the test with a significance level of 0.05. Linear fitting worked better and the difference in significance of one fit was less than 0.01. Under normal circumstances, when the temperature rose, the precipitation decreased. At the same time, when the temperature was lower than 11 °C, the precipitation decreased with the temperature rose. Combined with regional precipitation and temperature of the long-term inter-annual variation, in the 1990s of the fastest growing temperatures, the decline in precipitation was also greater. When a brief drop of temperature occurred in the 1970s, the precipitation also changed abruptly in 1968. Correlation between temperature and precipitation in the practice has been well confirmed.

5. Discussion

5.1. Different Methods for Investigating Temporal and Spatial Characteristics

This paper analyzed temporal and spatial characteristics of precipitation and temperature over the Beijing–Tianjin–Hebei region at the same time. The method used to convert surface rainfall made the results more accurate and representative. Different methods were mutual verification in the process of research, especially in the analysis of trend and abrupt change. The temporal trend of rainfall was

determined by cumulative anomaly method and EEMD method: the group of wet years and dry years occurred alternately, showing a decreasing trend in general. Hence, more than one abrupt point of precipitation could be found, which also confirmed the trend of precipitation. The Hurst index of precipitation was greater than 0.5, indicating that the precipitation may show a decreasing trend in the future. The continuous reduction in precipitation would result in higher demand for external water because the region had begun to supply the city from outside waters. At the same time, it is also extremely unfavorable for the task of restoration of over-exploitation of groundwater (Zhan et al. 2013). The analysis of concentration degree and concentration period analysis of precipitation helped to verify the occurrence time of the group of wet year and dry year, and analyze the time of annual wet season.

The temperature of this region in 54 years showed a significant upward trend at a rate of 0.26 °C/10 years. EEMD verified the accuracy of the study on the overall trend: the temperature rose sharply in the 1980s and 1990s. In addition, the nonparametric test method was used to verify abrupt change point by M–K method, showing that there was a significant difference in temperature before and after abrupt change. Wavelet analysis not only verified the cycle of temperature by EEMD, but also confirmed the variation trend of temperature and the correctness of the mutation point. The relationship between temperature and precipitation fitted by linear function was verified by a hypothesis of a significance level of 0.01. There was a very close relationship between temperature and precipitation in this region. The increase of temperature was likely to be accompanied by a reduction of rainfall, and this trend would continue in the future.

5.2. Cause of Characteristics of Precipitation and Temperature

As can be seen from the above studies, the precipitation and temperature in the Beijing–Tianjin–Hebei region has changed greatly in the past 50 years. The interaction of human activities, atmospheric circulation, the interaction of cold and warm atmosphere between sea and land were the main

reasons for the change of temperature and precipitation in the region (Mondal et al. 2012). When the region was controlled by a warm high-pressure system, it would, to some extent, block the transport of cold air from the Arctic to the region, which led to decrease of precipitation (Wang 2017). In addition, as China's political and cultural center, large number of fossils were fueled and forest has been heavily cut down. Large amounts of greenhouse gases absorbed the long wave radiation reflected by the earth. The process of urbanization accelerated and human increasing activities also led to a sudden increase in the region's temperature rise. Through the analysis of temperature by EOF method, the contribution rate of the two major cities (Beijing, Tianjin) was much higher than that in other regions to the temperature's rise. Huge electricity consumption and the rising proportion of the third industry led to an increase of temperature in Beijing when the temperature dropped temporarily in other area. Change of the sea level and the melting of the Arctic glaciers also led to the significant increase of temperature. The spatial variation of precipitation showed a decreasing trend from the southeast coastal areas to the northwest inland areas. In the wet years (1996, 1979), the water vapor carried by monsoon from the India ocean supplied the water vapor. Large water vapor flux transmission provided excellent conditions for a large number of precipitations in coastal regions (Wang 2017).

5.3. *Effects of the Temporal and Spatial Characteristic*

The increase of temperature and the decrease of rainfall in the Beijing–Tianjin–Hebei region will aggravate urban heat island effect. The period of 1996–2007 years was dry, when the annual average rainfall was significantly lower than the perennial, which led to a sharp reduction in reservoir water and rapid decline in groundwater levels. With the advance of precipitation concentration period, crops can basically meet the evapotranspiration demand in June and August of each year. However, due to the increase of temperature, it is necessary to advance the time and increase the amount of agricultural irrigation water. Because of the relationship between rainfall and air temperature in this area, the year of

high temperature may also be a year of water scarcity. Dry year has a great possibility to be the year of large water demand. This requires the water resources management department to seize the opportunity in the wet year to store water to supplement water supply in the dry years. Changes in climatic factors also have a profound impact on air quality of the region. There was a significant negative correlation between change of air pollution index and change of temperature in Beijing, Tianjin and Shijiazhuang, which indicated that the temperature had a significant positive effect on the air quality in the region.

6. *Conclusion*

In this paper, the results obtained by different methods were consistent. Through the analysis of precipitation and temperature in the Beijing–Tianjin–Hebei region, following conclusions were summarized:

1. From 1960 to 2013, precipitation showed a random downward trend. The annual average temperature showed a significant increasing trend at the rate of 0.26 °C/10 years. From the 1980s, the temperature underwent an abrupt change. In addition, the sequence of the temperature before and after the mutation passed through the significance test. The temperature changes can be divided to multiple time scales and the results of R/S analysis demonstrates that the temperature will continue to rise.
2. The coastal-inland difference was the main spatial distribution of precipitation in the region. As for temperature, the increasing trend of temperature in the Beijing-centered region and the area away from the sea is more pronounced. In terms of secondary vector fields, the striking feature is that the eastern coastal areas and high-altitude regions may have opposite trends with the temperature changes in the interior of the south.
3. Precipitation concentration and concentration period show strong spatial characteristics. The concentration degree of rainfall in the region was gradually reduced from the northeast to the

southwest in the spatial range and the concentration period became gradually earlier from south to north.

4. Precipitation and temperature show strong correlations in change. When temperature increased, the rainfall decreased. What is more, when the temperature mutated, the precipitation also changed rapidly.

Acknowledgements

This work was supported by the National Key R & D Program of China (Grant no. 2016YFC0401406).

Publisher's Note Springer Nature remains neutral with regard to jurisdictional claims in published maps and institutional affiliations.

REFERENCES

- Cheng, Q., Yan, Z., Wu, Z. H., et al. (2011). Trends in temperature extremes in association with weather-intrapersonal fluctuations in eastern China. *Advances in Atmospheric Science*, 28(2), 297–309.
- Ge, Q. S., Wang, H. J., Rutishauser, T., & Dai, J. (2015). Phenological response to climate change in China: A meta-analysis. *Global Change Biology*, 21(1), 265. <https://doi.org/10.1111/gcb.12648>.
- Golmohammadi, G., Rudra, R., Dickinson, T., et al. (2017). Predicting the temporal variation of flow contributing areas using SWAT. *Journal of Hydrology*, 547, 375–386.
- Jiang, R., Xie, J., Zhao, Y., et al. (2016). Spatiotemporal variability of extreme precipitation in Shaanxi province under climate change. *Theoretical and Applied Climatology*. <https://doi.org/10.1007/s00704-016-1910-y>.
- Jones, J. R., Schwartz, J. S., Ellis, K. N., et al. (2015). Temporal variability of precipitation in the Upper Tennessee Valley. *Journal of Hydrology: Regional Studies*, 3(C), 125–138.
- Kharin, V. V., Zwiers, F. W., Zhang, X., & Hegerl, G. C. (2013). Changes in temperature and precipitation extremes in the IPCC ensemble of global coupled model simulations. *Climatic Change*, 119(2), 345–357.
- Kundu, S., Khare, D., Mondal, A., et al. (2015). Analysis of spatial and temporal variation in rainfall trend of Madhya Pradesh, India (1901–2011). *Environmental Earth Sciences*, 73(12), 8197–8216. <https://doi.org/10.1007/s12665-014-3978-y>.
- Lee, D. K., Cha, D. H., & Jin, C. S. (2013). A regional climate change simulation over East Asia. *Asia-pacific Journal of Atmospheric Sciences*, 49(5), 655–664.
- Loukas, A., & Quick, M. C. (1996). Spatial and temporal distribution of storm precipitation in southwestern British Columbia. *Journal of Hydrology*, 174, 37–56.
- Meng, X. J., Zhang, S. J., & Zhang, Y. Y. (2013). Spatial and temporal variation of temperature and precipitation in Hexi Corridor. *Journal of geographical science*, 67(11), 1482–1492. **(In Chinese)**.
- Mondal, A., Khare, D., & Kundu, S. (2014). Spatial and temporal analysis of rainfall and temperature trend of India. *Theoretical and Applied Climatology*, 122(1–2), 143–158. <https://doi.org/10.1007/s00704-014-1283>.
- Mondal, A., Kundu, S., & Mukhopadhyay, A. (2012). Rainfall trend analysis by Mann-Kendall test: A case study of north-eastern part of Cuttack district, Orissa. *International Journal of Geology, Earth and Environmental Sciences*, 2(1), 70–78.
- Paola, F. D., & Giugni, M. (2013). Coupled spatial distribution of rainfall and temperature in USA. *Procedia Environmental Sciences*, 19(19), 178–187.
- Pavlik, D., Söhl, D., Pluntke, T., et al. (2012). Dynamic down-scaling of global climate projections for Eastern Europe with a horizontal resolution of 7 km. *Environmental Earth Sciences*, 65(5), 1475–1482.
- Qian, C., Ren, G., & Zhou, Y. (2016). Urbanization effects on climatic changes in 24 particular timings of the seasonal cycle in the middle and lower reaches of the Yellow River. *Theoretical and Applied Climatology*, 124(3–4), 781–791.
- Qin, Y., Yang, D. W., Lei, H. M., Xu, K., et al. (2015). Comparative analysis of drought based on precipitation and soil moisture indices in Haihe basin of North China during the period of 1960–2010. *Journal of Hydrology*, 526, 55–67. <https://doi.org/10.1016/j.jhydrol.2014.09.068>.
- Qiu, H. J., Cao, M. M., & Liu, W. (2011). Study on temporal and spatial variation of precipitation in Shaanxi Province Based on EOF. *Soil and water conservation bulletin*, 31(3), 57–59. **(In Chinese)**.
- Safavi, H. R., Sajjadi, S. M., & Raghibi, V. (2016). Assessment of climate change impacts on climate variables using probabilistic ensemble modeling and trend analysis. *Theoretical and Applied Climatology*. <https://doi.org/10.1007/s00704-016-1898-3>.
- Shi, Y. L., Cui, S. H., Ju, X. T., et al. (2015). Impacts of reactive nitrogen on climate change in China. *Scientific Reports*, 5, 8118. <https://doi.org/10.1038/srep08118>.
- Small, D., & Islam, S. (2006). Temporal invariance of leading EOFs for western United States precipitation over a range of scales. *Journal of Geophysical Research Atmospheres*, 111(D7), 1. <https://doi.org/10.1029/2005jd005876>.
- Västilä, K., Kummu, M., Sangmanee, C., et al. (2010). Modelling climate change impacts on the flood pulse in the Lower Mekong floodplains. *Journal of Water and Climate Change*, 1(1), 67–86. <https://doi.org/10.2166/wcc.2010.008>.
- Wang, G. (2017). Regional frequency analysis of observed sub-daily rainfall maxima over Eastern China. *Advances in Atmospheric Science*, 34(2), 209–225.
- Wang, J., Yan, Z. W., Liu, W. D., et al. (2013). Impact of urbanization on changes in temperature extremes in Beijing during 1978–2008. *Chinese Science Bulletin*, 58(36), 4679–4686.
- Wang, T., Zhang, M. C., Yu, Q. H., et al. (2012). Comparing the application of EMD and EEMD on time-frequency analysis of seismic signal. *Journal of Applied Geophysics*, 83(6), 29–34. <https://doi.org/10.1016/j.jappgeo.2012.05.002>.

- Xie, S. P., Xie, Q., Wang, D., et al. (2003). Summer upwelling in the South China Sea and its role in regional climate variations. *Journal of Geophysical Research Oceans*, 108(C8), 3261.
- Yang, P., Xia, J., Zhang, Y. Y., et al. (2017). Temporal and spatial variations of precipitation in Northwest China during 1960–2013. *Atmospheric Research*, 183, 283–295. <https://doi.org/10.1016/j.atmosres.2016.09.014>.
- Zhan, J., Huang, J., Zhao, T., et al. (2013). Modeling the impacts of urbanization on regional climate change: A case study in the Beijing–Tianjin–Tangshan metropolitan area. *Advances in Meteorology*, 7, 1–8. <https://doi.org/10.1155/2013/849479>.
- Zhang, X., Dai, Z., Chu, A., et al. (2014). Impacts of relative sea level rise on the shoreface deposition, Shuidong Bay, South China. *Environmental Earth Sciences*, 71(8), 3503–3515. <https://doi.org/10.1007/s12665-017-6418-y>.
- Zhou, T., Wu, B., & Dong, L. (2014). Advances in research of ENSO changes and the associated impacts on Asian-Pacific climate. *Asia-Pacific Journal of Atmospheric Sciences*, 50(4), 405–422.

(Received March 8, 2019, revised December 11, 2019, accepted December 17, 2019, Published online January 8, 2020)